On the Stress Distribution at the Base of a Stationary Crack[1]

By M. L. WILLIAMS,[2] PASADENA, CALIF.

In an earlier paper it was suggested that a knowledge of the elastic-stress variation in the neighborhood of an angular corner of an infinite plate would perhaps be of value in analyzing the stress distribution at the base of a V-notch. As a part of a more general study, the specific case of a zero-angle notch, or crack, was carried out to supplement results obtained by other investigators. This paper includes remarks upon the antisymmetric, as well as symmetric, stress distribution, and the circumferential distribution of distortion strain-energy density. For the case of a symmetrical loading about the crack, it is shown that the energy density is not a maximum along the direction of the crack but is one third higher at an angle $\pm \cos^{-1}(1/3)$; i.e., approximately ±70 deg. It is shown that at the base of the crack in the direction of its prolongation, the principal stresses are equal, thus tending toward a state of (two-dimensional) hydrostatic tension. As the distance from the point of the crack increases, the distortion strain energy increases, suggesting the possibility of yielding ahead of the crack as well as ±70 deg to the sides. The maximum principal tension stress occurs on ±60 deg rays. For the antisymmetrical stress distribution the distortion strain energy is a relative maximum along the crack and 60 per cent lower ± 85 deg to the sides.

MANY previous investigators have studied the elastic-stress distributions around cracks with some of the earliest contributions being from Inglis (1)[3] who studied an internal crack using elliptical bounding surfaces, Griffith (2) who set up an energy criterion for crack instability, Westergaard who initially treated the crack problem in the same way to be exploited in this paper (3), as well as by the complex variable technique in a later paper (4). The stress distribution at the base of cracks also has been examined photoelastically with the first attempt to measure isochromatic-fringe patterns in this specific application apparently being accomplished by Hollister (5). Recently Post (6) has published some interesting results of his photoelastic observations for the case of an edge crack.

It is the purpose of this paper to supplement the results of these investigators in certain respects which it is hoped will aid in the further understanding of the elastic-stress distribution at the base of a stationary crack.

[1] This investigation was sponsored in part by the National Advisory Committee for Aeronautics, under Contract NAw-6431.

[2] Associate Professor, California Institute of Technology.

[3] Numbers in parentheses refer to the Bibliography at the end of the paper.

Contributed by the Applied Mechanics Division and presented at the Annual Meeting, New York, N. Y., November 25–30, 1956, of THE AMERICAN SOCIETY OF MECHANICAL ENGINEERS.

Discussion of this paper should be addressed to the Secretary, ASME, 29 West 39th Street, New York, N. Y., and will be accepted until April 10, 1957, for publication at a later date. Discussion received after the closing date will be returned.

NOTE: Statements and opinions advanced in papers are to be understood as individual expressions of their authors and not those of the Society. Manuscript received by ASME Applied Mechanics Division, March 21, 1956. Paper No. 56—A-16.

In a previous investigation (7) the plane-stress distribution near the vertex of an infinite sector of included angle α was considered for various combinations of boundary conditions. For the particular purpose of this paper it is desired to consider the case where the two radial edges of the plate are unloaded and the included angle approaches 2π. It has been shown that stress functions, i.e., solutions of $\nabla^4\chi(r, \theta) = 0$, of the form

$$\chi(r, \theta, \lambda) \equiv r^{\lambda+1}F(\theta; \lambda) = r^{\lambda+1}[c_1 \sin(\lambda + 1)\theta + c_2 \cos(\lambda + 1)\theta + c_3 \sin(\lambda - 1)\theta + c_4 \cos(\lambda - 1)\theta] \quad [1]$$

will satisfy the conditions of stress-free edges along $\theta = 0$ and $\theta = \alpha$ if the λ are chosen as the positive roots of

$$\sin(\lambda\alpha) = \pm\lambda \sin\alpha \quad [2]$$

For the case where $\alpha = 2\pi$, corresponding to the case of a crack with flank angle $\omega = \alpha - 2\pi = 0$, the eigenequation takes the particularly simple form $\sin(2\pi\lambda) = 0$, thus requiring $\lambda = n/2$, $n = 1, 2, 3, \ldots$, and yielding the stress function

$$\chi(r, \theta; n/2) = r^{(n/2)+1}\left[c_1 \sin\left(\frac{n}{2} + 1\right)\theta + c_2 \cos\left(\frac{n}{2} + 1\right)\theta + c_3 \sin\left(\frac{n}{2} - 1\right)\theta + c_4 \cos\left(\frac{n}{2} - 1\right)\theta\right] \quad [3]$$

From the general definition of the stress function

$$\sigma_r = \frac{1}{r^2}\frac{\partial^2\chi}{\partial\theta^2} + \frac{1}{r}\frac{\partial\chi}{\partial\theta} = r^{\lambda-1}[F''(\theta) + (\lambda + 1)F(\theta)] \quad [4]$$

$$\sigma_\theta = \frac{\partial^2\chi}{\partial r^2} = r^{\lambda-1}[\lambda(\lambda + 1)F(\theta)] \quad [5]$$

$$\tau_{r\theta} = -\frac{1}{r}\frac{\partial^2\chi}{\partial r\partial\theta} + \frac{1}{r^2}\frac{\partial\chi}{\partial\theta} = r^{\lambda-1}[-\lambda F'(\theta)] \quad [6]$$

one proceeds to require for this case that σ_θ and $\tau_{r\theta}$ vanish on $\theta = 0$ and $\theta = \alpha = 2\pi$. By reference to Equations [3–6] this implies that

$$F(0, n/2) = F'(0, n/2) = F(2\pi, n/2) = F'(2\pi, n/2) = 0$$

Ordinarily, that is, if $\alpha < 2\pi$, the four homogeneous boundary conditions permit three of the four c_i constants to be determined in terms of the fourth. In this case, however, all four boundary conditions can be satisfied by

$$\chi(r, \theta) = r^{(n/2)+1}\left\{c_3\left[\sin\left(\frac{n}{2} - 1\right)\theta - \frac{n-2}{n+2}\sin\left(\frac{n}{2} + 1\right)\theta\right] + c_4\left[\cos\left(\frac{n}{2} - 1\right)\theta - \cos\left(\frac{n}{2} + 1\right)\theta\right]\right\} \quad [7]$$

where the first term is equivalent to that used by Westergaard (3).

Turning now to a more convenient alternate form of expressing Equation [7] in terms of the bisector angle $\psi = \theta - \pi$, the stress

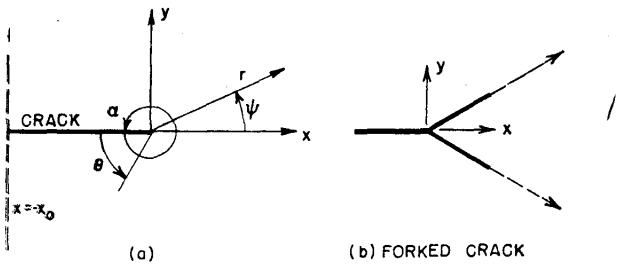

FIG. 1 GEOMETRY

function $\chi(r, \psi)$ can be split into its even $\chi_e(r, \psi)$ and odd $\chi_0(r, \psi)$ parts with respect to ψ (Fig. 1)

$$\chi_e(r, \psi) = \sum_{n = 1, 2, 3, \ldots} \left\{ (-1)^{n-1} a_{2n-1} r^{n+\frac{1}{2}} \left[-\cos\left(n - \frac{3}{2}\right)\psi + \frac{2n-3}{2n+1} \cos\left(n + \frac{1}{2}\right)\psi \right] + (-1)^n a_{2n} r^{n+1} \left[-\cos\left(n - \frac{3}{2}\right)\psi + \cos\left(n + \frac{1}{2}\right)\psi \right] \right\} \quad [8]$$

$$\chi_0(r, \psi) = \sum_{n = 1, 2, 3, \ldots} \left\{ (-1)^{n-1} b_{2n-1} r^{n+\frac{1}{2}} \left[\sin\left(n - \frac{3}{2}\right)\psi - \sin\left(n + \frac{1}{2}\right)\psi \right] + (-1)^n b_{2n} r^{n+1} \left[-\sin\left(n - \frac{3}{2}\right)\psi + \frac{2n-3}{2n+1} \sin\left(n + \frac{1}{2}\right)\psi \right] \right\} \quad [9]$$

It should be observed that even though the field equation and the boundary conditions along the radial edges are satisfied, the constants a_i and b_i are undetermined. Their values of course depend upon the loading conditions; more specifically, either upon the boundary conditions at infinity in the case of an infinite sector, or upon those at some fixed radius when the plate has finite dimensions. For the latter practical case, which includes the problem under consideration, all the higher eigenfunctions in general will be present in order to determine a solution in the large.

Upon writing out the first few terms

$$\chi(r, \psi) = r^{3/2} \left[a_1 \left(-\cos\frac{\psi}{2} - \frac{1}{3}\cos\frac{3\psi}{2} \right) + b_1 \left(-\sin\frac{\psi}{2} - \sin\frac{3\psi}{2} \right) \right] + a_2 r^2 [1 - \cos 2\psi] + 0(r^{5/2}) + \ldots \quad [10]$$

from which the associated stresses may be found from Equations [4–6] as

$$\sigma_r(r, \psi) = \frac{1}{4r^{1/2}} \left\{ a_1 \left[-5\cos\frac{\psi}{2} + \cos\frac{3\psi}{2} \right] + b_1 \left[-5\sin\frac{\psi}{2} + 3\sin\frac{3\psi}{2} \right] \right\} + 4a_2 \cos^2\psi + 0(r^{1/2}) + \ldots \quad [11]$$

$$\sigma_\psi(r, \psi) = \frac{1}{4r^{1/2}} \left\{ a_1 \left[-3\cos\frac{\psi}{2} - \cos\frac{3\psi}{2} \right] + b_1 \left[-3\sin\frac{\psi}{2} - 3\sin\frac{3\psi}{2} \right] \right\} + 4a_2 \sin^2\psi + 0(r^{1/2}) + \ldots \quad [12]$$

$$\tau_{r\psi}(r, \psi) = \frac{1}{4r^{1/2}} \left\{ a_1 \left[-\sin\frac{\psi}{2} - \sin\frac{3\psi}{2} \right] + b_1 \left[\cos\frac{\psi}{2} + 3\cos\frac{3\psi}{2} \right] \right\} - 2a_2 \sin 2\psi + 0(r^{1/2}) + \ldots \quad [13]$$

Before proceeding further, it is convenient to identify the stress state which is multiplied by the constant a_2, viz.

$$a_2 r^2(1 - \cos 2\psi) = 2a_2 r^2 \sin^2\psi = 2a_2 y^2$$

In the Cartesian co-ordinates analog of Equations [4–6], the stresses are

$$\sigma_x = 4a_2, \quad \sigma_y = 0, \quad \text{and } \tau_{xy} = 0$$

For most cases of interest, including the usual tension and bending specimens, σ_x along the edge $x = -x_0$ (see Fig. 1) is zero; hence for these cases $\sigma_x = 4a_2 = 0$ and thus Equations [11–13] with respect to the radial variation are all of the form $r^{-1/2} + 0(r^{1/2})$, and the local stress variations in the vicinity of the base of the crack, $r \to 0$, are proportional, up to vanishing terms in r, to the contribution of the first term. If the boundary $x = -x_0$ were loaded, however, say by a uniform pressure, this contribution would have to be superimposed.

It is convenient at this point to compute two quantities useful in photoelastic analysis; specifically, the sum of the normal stresses, which is proportional to the isopachic lines, and the difference of the principal stresses, which is proportional to the isochromatic lines.

Thus

$$\sigma_r + \sigma_\psi = \frac{1}{4r^{1/2}} \left\{ a_1 \left[-8\cos\frac{\psi}{2} \right] + b_1 \left[-8\sin\frac{\psi}{2} \right] \right\} + \ldots = \sigma_1 + \sigma_2 \quad [14]$$

$$\sigma_1 - \sigma_2 = [(\sigma_r - \sigma_\psi)^2 + 4\tau_{r\psi}^2]^{1/2} = \frac{\pm 1}{4r^{1/2}} \left\{ 16a_1^2 \sin^2\psi + 64b_1^2 \left(1 - \frac{3}{4}\sin^2\psi \right) \right\}^{1/2} + \ldots \quad [15]$$

The direction of principal stress is found from the condition that the shear stress, τ_{ns}, on a plane whose normal is inclined at an angle α to the radius vector vanishes

$$\tau_{ns} = \tau_{r\psi}\cos 2\alpha - (1/2)(\sigma_r - \sigma_\psi)\sin 2\alpha = 0$$

$$0 = -r^{-1/2} \left\{ \left[\sin\frac{\psi}{2}\cos^2\frac{\psi}{2}\cos 2\alpha - \cos\frac{\psi}{2}\sin^2\frac{\psi}{2}\sin 2\alpha \right] a_1 + \left[\cos\frac{\psi}{2}\left(2 - 3\cos^2\frac{\psi}{2} \right)\cos 2\alpha + \sin\frac{\psi}{2}\left(2 - 3\sin^2\frac{\psi}{2} \right)\sin 2\alpha \right] b_1 \right\} + \ldots \quad [16]$$

The angle β of a stress trajectory with the x-axis, Fig. 1, is then $\beta = \psi + \alpha$. Also the total strain-energy density

$$W = \frac{1}{2E}\left[\sigma_r^2 + \sigma_\psi^2 - 2\nu\sigma_r\sigma_\psi + 2(1+\nu)\tau_{r\psi}^2\right] \ldots [17]$$

and the strain energy due to distortion alone, i.e., the total strain energy less that due to change in volume

$$W_d = \frac{1}{12G}\left[(\sigma_1 - \sigma_2)^2 + (\sigma_2 - \sigma_3)^2 + (\sigma_3 - \sigma_1)^2\right] = \frac{1}{12G}(3\tau_{oct})^2 \ldots [18]$$

where the expression is given in terms of principal stresses ($\sigma_3 = 0$ in this case), and the definition of the octahedral shearing stress has been used, may be written, respectively, as

$$32ErW = a_1^2\left[(34 - 30\nu)\cos^2\frac{\psi}{2} + 2(1+\nu)\sin^2\frac{\psi}{2} + 2(1+\nu) - 4(1+\nu)\cos 2\psi\right] + b_1^2\left[(34 - 30\nu)\sin^2\frac{\psi}{2} + 2(1+\nu)\cos^2\frac{\psi}{2} + 18(1+\nu) + 12(1+\nu)\cos 2\psi\right] + 2a_1b_1\left[(32 - 22\nu)\sin\frac{\psi}{2}\cos\frac{\psi}{2} - 8(1+\nu)\sin 2\psi\right] + \ldots [19]$$

$$6GrW_d = a_1^2\left(1 + 3\sin^2\frac{\psi}{2}\right)\cos^2\frac{\psi}{2} + 2b_1^2\left[3 + \left(1 + 3\cos\frac{\psi}{2}\right)\left(1 - 3\cos\frac{\psi}{2}\right)\sin^2\frac{\psi}{2}\right] + 2a_1b_1\sin\psi + \ldots [20]$$

In the foregoing expressions it is seen that the term multiplied by the coefficient a_1b_1 represents a coupling between the symmetric and antisymmetric variations with respect to ψ.

Finally, the displacements (see reference 7) are found to be

$$2\mu U_r(r,\psi) = r^{1/2}\left\{a_1\left[\left(-\frac{5}{2} + 4\sigma\right)\cos\frac{\psi}{2} + \frac{1}{2}\cos\frac{3\psi}{2}\right] + b_1\left[(-3 + 4\sigma)\sin\frac{\psi}{2} + \sin\frac{3\psi}{2}\right]\right\} + \ldots [21]$$

$$2\mu U_\psi(r,\psi) = r^{1/2}\left\{a_1\left[\left(\frac{7}{2} - 4\sigma\right)\sin\frac{\psi}{2} - \frac{1}{2}\sin\frac{3\psi}{2}\right] + b_1\left[-\left(\frac{7}{2} - 4\sigma\right)\cos\frac{\psi}{2} + \frac{3}{2}\cos\frac{3\psi}{2}\right]\right\} + \ldots [22]$$

where

$$\sigma \equiv \nu/(1+\nu)$$

Symmetrical Stress Distribution

For the sake of simplicity it is convenient to analyze the two types of solutions separately; the symmetric solutions, i.e., $b_i = 0$, are perhaps the more common, occurring, for example, in the case of an edge crack in a thin plate subjected to bending or tension.

Specializing the stresses and the other quantities to this case gives

$$\sigma_r(r,\psi) = \frac{1}{4r^{1/2}}\left[-5\cos\frac{\psi}{2} + \cos\frac{3\psi}{2}\right]a_1 + \ldots [23]$$

$$\sigma_\psi(r,\psi) = \frac{1}{4r^{1/2}}\left[-3\cos\frac{\psi}{2} - \cos\frac{3\psi}{2}\right]a_1 + \ldots [24]$$

$$\tau_{r\psi}(r,\psi) = \frac{1}{4r^{1/2}}\left[-\sin\frac{\psi}{2} - \sin\frac{3\psi}{2}\right]a_1 + \ldots [25]$$

$$2\mu U_r(r,\psi) = r^{1/2}\left[\left(-\frac{5}{2} + 4\sigma\right)\cos\frac{\psi}{2} + \frac{1}{2}\cos\frac{3\psi}{2}\right]a_1 + \ldots [26]$$

$$2\mu U_\psi(r,\psi) = r^{1/2}\left[\left(\frac{7}{2} - 4\sigma\right)\sin\frac{\psi}{2} - \frac{1}{2}\sin\frac{3\psi}{2}\right]a_1 + \ldots [27]$$

$$\sigma_1 + \sigma_2 = \frac{1}{4r^{1/2}}\left[-8\cos\frac{\psi}{2}\right]a_1 + \ldots [28]$$

$$\sigma_1 - \sigma_2 = \frac{1}{4r^{1/2}}\left[4a_1\sin\psi\right] + \ldots [29]$$

$$\beta_{n=1} = (3\psi/4) \pm (\pi/4);\ \text{also isotropic locus at } \psi = 0 \ldots [30]$$

$$W = \frac{a_1^2}{Er}\cos^2\frac{\psi}{2}\left[1 - \nu + (1+\nu)\sin^2\frac{\psi}{2}\right] + \ldots [31]$$

$$W_d = \frac{a_1^2}{Er}\cos^2\frac{\psi}{2}\left[\frac{1+\nu}{3} + (1+\nu)\sin^2\frac{\psi}{2}\right] + \ldots [32]$$

It is observed that, for this elastic behavior in an isotropic homogeneous material, the stress system represented by the first term possesses the characteristic square-root singularity found by Inglis (1), Westergaard (4), and others; also, the shapes of the isopachics and isochromatic fringes are in agreement with photoelastic data obtained by Post (6) and corroborated independently at GALCIT. In addition, however, there are certain other interesting features which, because of the relative simplicity of the previous expressions, become readily apparent.

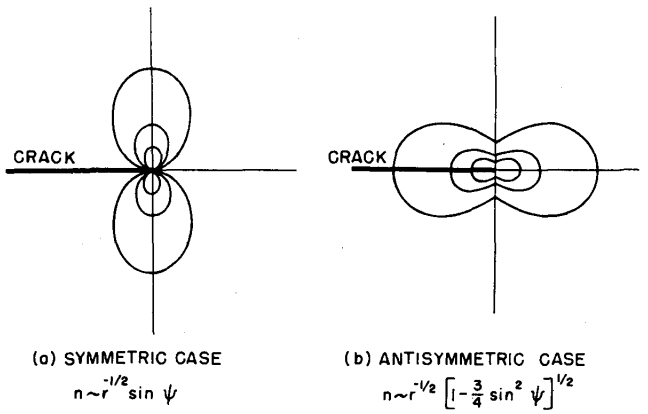

Fig. 2 Isochromatic-Fringe Patterns

The first of these relates to the observation that the shear stress is zero along the line of propagation of the crack ($\psi = 0$). The σ_r and σ_ψ stresses must therefore be principal stresses as expected, but moreover from Equation [29] the stresses are equal

$$\sigma_1(0) \rightarrow \sigma_2(0) = (-a_1)r^{-1/2} + \ldots$$

In other words, at the base of the crack there exists a strong tend-

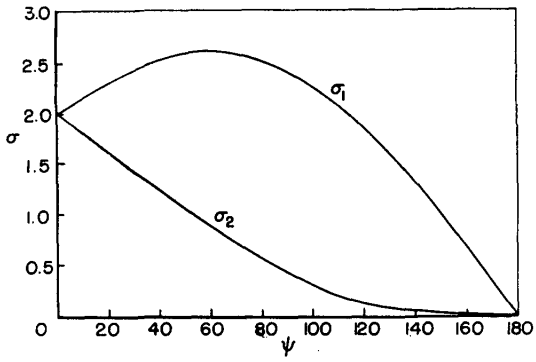

(a) SYMMETRIC CASE

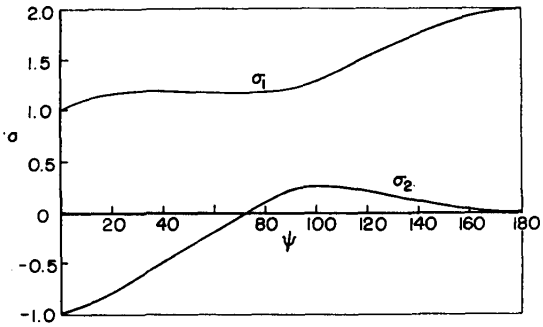

(b) ANTISYMMETRIC CASE

FIG. 3 PRINCIPAL-STRESS VARIATIONS

ency toward a state of (two-dimensional) hydrostatic tension which consequently may permit the elastic analysis to apply closer to the point of the crack that was hitherto supposed, notwithstanding the square-root stress singularity.

In order to investigate this point a bit more fully, particularly for the higher terms in r, i.e., further away from the crack point, more terms can be considered in Equations [23] and [24] to obtain, for $\psi = 0$

$$\sigma_r(r, 0) = \sum_{n = 1, 2, 3 \ldots} (-1)^n (2n - 1) a_{2n-1} r^{n - \frac{3}{2}} \quad [33]$$

$$\sigma_\psi(r, 0) = \sum_{n = 1, 2, 3 \ldots} \left\{ (-1)^n (2n - 1) a_{2n-1} r^{n - \frac{3}{2}} + (-1)^{n+1} 2a_{2n} (2n - 1) r^{n-1} \right\} \quad [34]$$

from which it may be concluded that, if the constant loading term $a_2 = 0$, the principal stresses are equal up to the linear term in r. From the previous relation the difference between the stresses can then be written

$$\sigma_r - \sigma_\psi = \sum_{n = 1, 2, 3 \ldots} (-1)^n 2a_{2n} (2n - 1) r^{n-1} \quad [35]$$

Therefore the principal stresses will become progressively unequal and the tendency toward hydrostatic tension reduced as the distance from the crack increases. As a matter of interest the stress trajectories for the lowest eigensolution, $n = 1$, are shown in Fig. 5 and they are observed to be of the interlocking type which explains the apparent contraction that $\beta = \pm\pi/4$ for $\psi = 0$ from

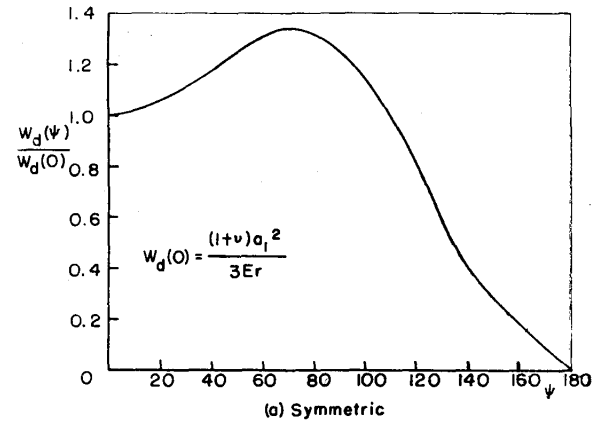

(a) Symmetric

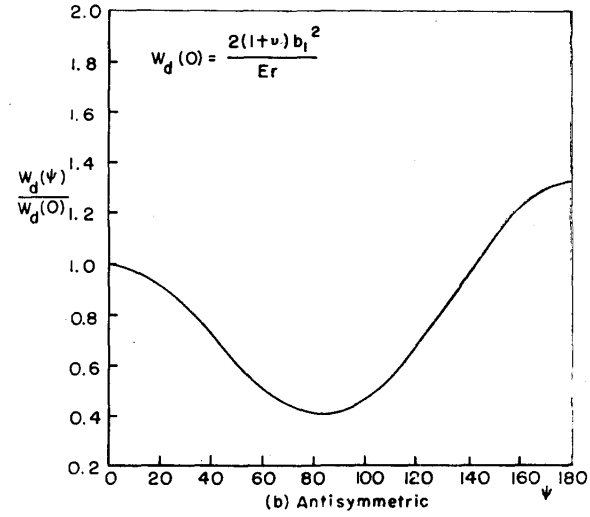

(b) Antisymmetric

FIG. 4 STRAIN-ENERGY-DENSITY DISTRIBUTIONS

Equation [30]. The equality of the principal stresses leads to a locus of isotropic points.

Another interesting characteristic of the solution is shown in Fig. 4 which shows the variation of distortion strain energy as a function of angle for a fixed radius. Because of the afore-mentioned hydrostatic tendency, the maximum energy of distortion does not occur along the line of crack direction, but rather at

$$\psi^* = \pm\cos^{-1}(1/3) \approx \pm 70 \text{ deg}$$

where it is one third higher.

The previous results also give the principal stress as

$$\sigma_{1,2} = -\frac{a_1}{r^{1/2}} \cos\frac{\psi}{2} \left[1 \mp \sin\frac{\psi}{2} \right]$$

for which the maximum value of $(3\sqrt{3}/4)(-a_1)r^{-1/2}$ occurs at $\bar{\psi} = \cos^{-1}(1/2) = \pi/3$ at which angle the stress trajectories are parallel to the x, y-co-ordinates; i.e., $\beta = 0, \pi/2$. The maximum shear stress $\tau_{max} = 1/2\,(\sigma_1 - \sigma_2)$ oriented at $\beta = \pi/8, 5\pi/8$, $\psi = \pi/2$ and equals exactly one half the hydrostatic tension value to which the normal stresses are subjected along $\psi = 0$ at the same radial distance. Some of the foregoing properties are summarized in Fig. 6.

Finally, the radial and circumferential displacements on the free edges from Equations [23] and [24] are found to be zero and $\pm 4(1 + \nu)^{-1} a_1 r^{1/2}$, thus leading to the expected fact that the two faces will have closed together and overlapped under a compression loading, an impossible situation by itself requiring $a_1 = 0$.

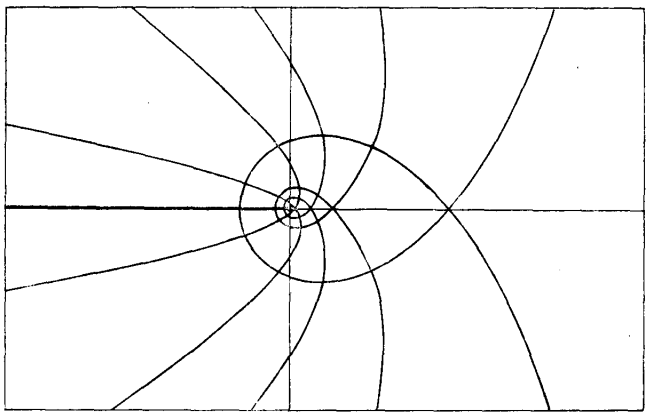

FIG. 5 STRESS TRAJECTORIES FOR LOWEST EVEN EIGENFUNCTION $\beta = (3\psi/4) \pm (\pi/4)$

In this case one is led to the contact problem treated by Westergaard (4) wherein there is no stress singularity at the point of the crack.

ANTISYMMETRICAL STRESS DISTRIBUTION

When the stress distribution is antisymmetric, which is a case that does not seem previously to have been treated explicitly, such as may exist about a crack parallel to the neutral axis of a beam in pure bending, there results

$$\sigma_r(r, \psi) = \frac{1}{4r^{1/2}}\left[-5 \sin^2 \frac{\psi}{2} + 3 \sin \frac{3\psi}{2}\right] b_1 + \ldots \ldots [36]$$

$$\sigma_\psi(r, \psi) = \frac{1}{4r^{1/2}}\left[-3 \sin \frac{\psi}{2} - 3 \sin \frac{3\psi}{2}\right] b_1 + \ldots \ldots [37]$$

$$\tau_{r\psi}(r, \psi) = \frac{1}{4r^{1/2}}\left[\cos \frac{\psi}{2} + 3 \cos \frac{3\psi}{2}\right] b_1 + \ldots \ldots [38]$$

$$2\mu U_r(r, \psi) = r^{1/2}\left[(-3 + 4\sigma) \sin \frac{\psi}{2} + \sin \frac{3\psi}{2}\right] b_1 + \ldots \ldots [39]$$

$$2\mu V_\psi(r, \psi) = r^{1/2}\left[-\left(\frac{7}{2} - 4\sigma\right)\cos \frac{\psi}{2} + \frac{3}{2} \cos \frac{3\psi}{2}\right] b_1 + \ldots \ldots [40]$$

$$\sigma_1 + \sigma_2 = \frac{1}{4r^{1/2}}\left[-8 \sin \frac{\psi}{2}\right] b_1 + \ldots \ldots [41]$$

$$\sigma_1 - \sigma_2 = \frac{1}{4r^{1/2}}\left[8\left(1 - \frac{3}{4} \sin^2 \psi\right)^{1/2}\right] b_1 + \ldots \ldots [42]$$

$$W = \frac{b_1^2}{Er}\left[(1 - \nu) \sin^2 \frac{\psi}{2} + (1 + \nu)\left(1 - \frac{3}{4} \sin^2 \psi\right)\right] + \ldots \ldots [43]$$

$$W_d = \frac{b_1^2}{Er}\left[\frac{1 + \nu}{3} \sin^2 \frac{\psi}{2} + (1 + \nu)\left(1 - \frac{3}{4} \sin^2 \psi\right)\right] + \ldots \ldots [44]$$

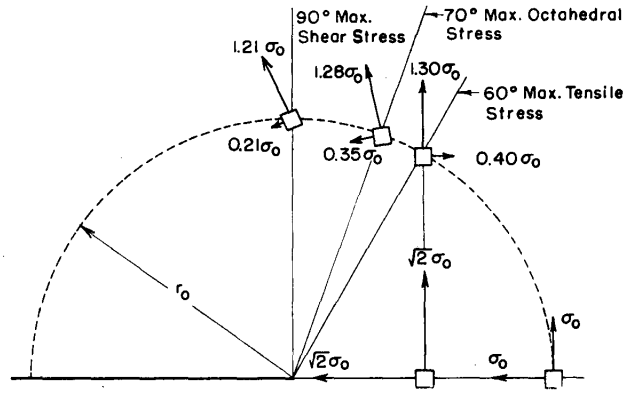

FIG. 6 CRITICAL PRINCIPAL STRESSES FOR THE LOWEST EVEN EIGENFUNCTION $\sigma_0 = -a_1 r_0^{-1/2}$

Again in this case the singular stress system varies as $r^{-1/2}$; the distortion-strain-energy-density variation is shown in Fig. 4. It is interesting to observe that in this case the energy drops on either side from a relative maximum in the direction of the crack to a minimum of 40 per cent of its $\psi = 0$ value at $\psi^* = \cos^{-1}(1/9)$.

It would be interesting to experiment photoelastically with the antisymmetric-loading condition, which is not too simple a matter, in an analysis similar to that of Post for the symmetrical case.

CONCLUSION

While it is not the intent to extend the range of validity of the elastic analysis by delving into the complicated phenomenon of failure or fracture mechanics, it does seem pertinent to remark upon some possible implications of the results obtained from elasticity theory.

First of all it seems that even in the presence of a partial (two-dimensional) hydrostatic-stress field there would be a reduced tendency for yielding at the base of the crack. Then, as the magnitude of the individual stresses increases as the inverse half power of the radius, the stress should become quite high with a tendency toward a cleavage failure. At the same time the elastic analysis indicates there should be a large amount of distortion off to the sides of the crack and presumably some yielding should take place in these areas which would tend toward a ductile failure. The character of failure actually occurring in a given specimen would depend upon the material. In this connection it is pertinent to mention some recent experimental evidence of Forsyth and Stubbington (8) called to the author's attention by S. R. Valluri, which tends to substantiate the remarks concerning an area of yielding off the crack direction, presumably ±70 deg for an exactly symmetrical loading.

In addition, because the stress becomes nonhydrostatic as the distance from the point of the crack increases, by Equation [35], there may be reason therefore to suspect a yielded region ahead of the crack also, although not as severe.

As a second remark, concerning the direction of cracking or forking, it is recognized that slow-moving cracks generally propagate more or less straight.[4] Because some cracks do fork,

[4] In an interesting piece of work Yoffe (9) has discussed the change of direction of a running crack due to its velocity and has found that if the material is such that a crack propagates in a direction normal to the maximum tensile stress (which, incidentally, is not σ_ψ as she apparently has assumed; indeed aside from the principal stresses, $\sigma_r \geq \sigma_\psi$), there is a critical velocity of about 0.6 times the velocity of shear waves in the material above which the crack tends to become curved. It may be of value to supplement her work by testing her hypothesis with respect to the maximum principal tensile stress; it is suspected, however, that the results will be qualitatively the same because, as she has remarked and as is shown in Fig. 6, the stress field is relatively uniform over a wide area in front of the crack.

however, it may be worth noting that any arbitrary crack will be subjected simultaneously to both symmetric and antisymmetric loading. In this connection it is observed that for the antisymmetric contributions the relative maximum and minimum energies, for example, tend to negate the effects which occur for a symmetrical loading. One might therefore conclude that for randomly oriented cracks there would be no preferred direction that the crack might take upon moving, with macroscopic structure and rate-of-energy release being controlling factors. On the other hand, it may be possible to relate the maximum principal tensile stresses occurring at ± 60 deg, in the neighborhood of the maximum distortion, to the angle crack-forking phenomenon shown, for example, by Post (6) or in Fig. 1(*b*), although again for metals as opposed to plastics the effect of crystal orientation and slip planes probably would be quite strong.

BIBLIOGRAPHY

1 "Stresses in a Plate Due to the Presence of Cracks and Sharp Corners," by C. E. Inglis, Transactions of the Institution of Naval Architects, London, England, vol. 60, 1913, p. 219.

2 "The Phenomena of Rupture and Flow in Solids," by A. A. Griffith, Philosophical Transactions of the Royal Society of London, England, vol. 221, 1921, pp. 163–198.

3 "Stresses at a Crack, Size of the Crack and the Bending of Reinforced Concrete," by H. M. Westergaard, Proceedings of the American Concrete Institute, vol. 30, 1934, pp. 93–102.

4 "Bearing Pressures and Cracks," by H. M. Westergaard, JOURNAL OF APPLIED MECHANICS, Trans. ASME, vol. 61, 1939, pp. A-49-53.

5 "Experimental Study of Stresses at a Crack in a Compression Member," by S. C. Hollister, Proceedings of the American Concrete Institute, vol. 30, 1934, pp. 361–365.

6 "Photoelastic Stress Analysis for an Edge Crack in a Tensile Field," by D. Post, Proceedings of the Society for Experimental Stress Analysis, vol. 12, no. 1, 1954, p. 99.

7 "Stress Singularities Resulting From Various Boundary Conditions in Angular Corners of Plates in Extension," by M. L. Williams, JOURNAL OF APPLIED MECHANICS, Trans. ASME, vol. 74, 1952, p. 526.

8 "The Slip Band Extrusion Effect Observed in Some Aluminum Alloys Subjected to Cyclic Stresses," by P. J. E. Forsyth and C. A. Stubbington, Royal Aircraft Establishment, MET Report 78, January, 1954.

9 "The Moving Griffith Crack," by E. H. Yoffe, *Philosophical Magazine*, vol. 42, part 2, 1951, pp. 739–750.